

Electron Spin Polarization in Resonant Interband Tunneling Devices

A. G. Petukhov^{1,2}, D. O. Demchenko^{2 *}, and A. N. Chantis^{2†}

¹*Center for Computational Materials Science,*

Naval Research Laboratory, Washington, DC 20375

²*Physics Department, South Dakota School of Mines and Technology, Rapid City, SD 57701*

(Dated: February 1, 2008)

Abstract

We study spin-dependent interband resonant tunneling in double-barrier InAs/AlSb/Ga_xMn_{1-x}Sb heterostructures. We demonstrate that these structures can be used as spin filters utilizing spin-selective tunneling of electrons through the light-hole resonant channel. High densities of the spin polarized electrons injected into bulk InAs make spin resonant tunneling devices a viable alternative for injecting spins into a semiconductor. Another striking feature of the proposed devices is the possibility of inducing additional resonant channels corresponding to the heavy holes. This can be implemented by saturating the in-plane magnetization in the quantum well.

PACS numbers: 75.70.Pa, 73.40.Gk, 75.50.Pp, 85.75.Mm

* Present address: Physics Department, Georgetown University, Washington, DC 20057

† Present address: Department of Chemical and Materials Engineering, Arizona State University, Tempe, AZ 85287

One of the goals and challenges of the modern spintronics is the ability to create stable sources of spin polarized electrons that can be injected into the bulk of a semiconductor. One way of achieving this goal is to inject spins from a ferromagnetic metal into a semiconductor through a Schottky barrier [1, 2, 3]. Another alternative consists in using all-semiconductor spin filtering devices. One class of the proposed spin-filters utilizes the Rashba effect in double-well resonant tunneling structures [4]. Another class of these devices uses inter-band (or Zener) spin-dependent tunneling in heterostructures comprising nonmagnetic and magnetic semiconductors [5, 6]. The utilization of Zener tunneling in structures based on epitaxially grown III-V dilute magnetic semiconductors (DMS) is a necessary logical step in designing all-semiconductor spin injection devices. Indeed, it has been proven experimentally that the electrons in III-V semiconductors have remarkably long spin lifetimes while the holes tend to rapidly dissipate their spin [7]. Therefore, for further spin manipulations, one needs the spin-polarized electrons rather than the holes, while to date all known III-V DMS are *p*-type. The first spin-injection devices (Esaki diodes) based on Zener tunneling of valence electrons from *p*-type ferromagnetic GaMnAs into *n*-GaAs have been already fabricated and successfully tested [5, 6].

In this Letter we consider theoretically another type of system that utilizes spin-dependent *resonant* tunneling in magnetic heterostructures with type-II broken-gap band alignment. These systems are resonant interband tunneling devices (RITD) based on InAs/AlSb/GaMnSb/AlSb/InAs double-barrier heterostructures (DBH). A schematic band diagram of such a DBH is shown in the inset to Fig.1. The band offset between InAs and GaMnSb leaves a 0.15 eV energy gap between the bottom of the conduction band in InAs and top of valence band in GaMnSb [8]. Therefore the electrons from InAs emitter can tunnel through the hole states in the GaMnSb quantum well into InAs collector. Since the quantized hole states in the quantum well are spin-polarized the emerging electrons are expected to be spin-polarized as well. Previous investigations of conventional (i. e. spin-independent) interband resonant tunneling have been mainly focused on RITDs with GaSb quantum wells [8, 9] or similar devices [10, 11, 12] and revealed quite robust operation in a wide temperature range.

The spin-filtering effect, or more precisely, the exchange splitting of the light-hole channel has been observed experimentally in DBH with semimetallic ErAs quantum wells [13]. The band diagram of the ErAs-based system is similar to that of the proposed GaMnSb-based

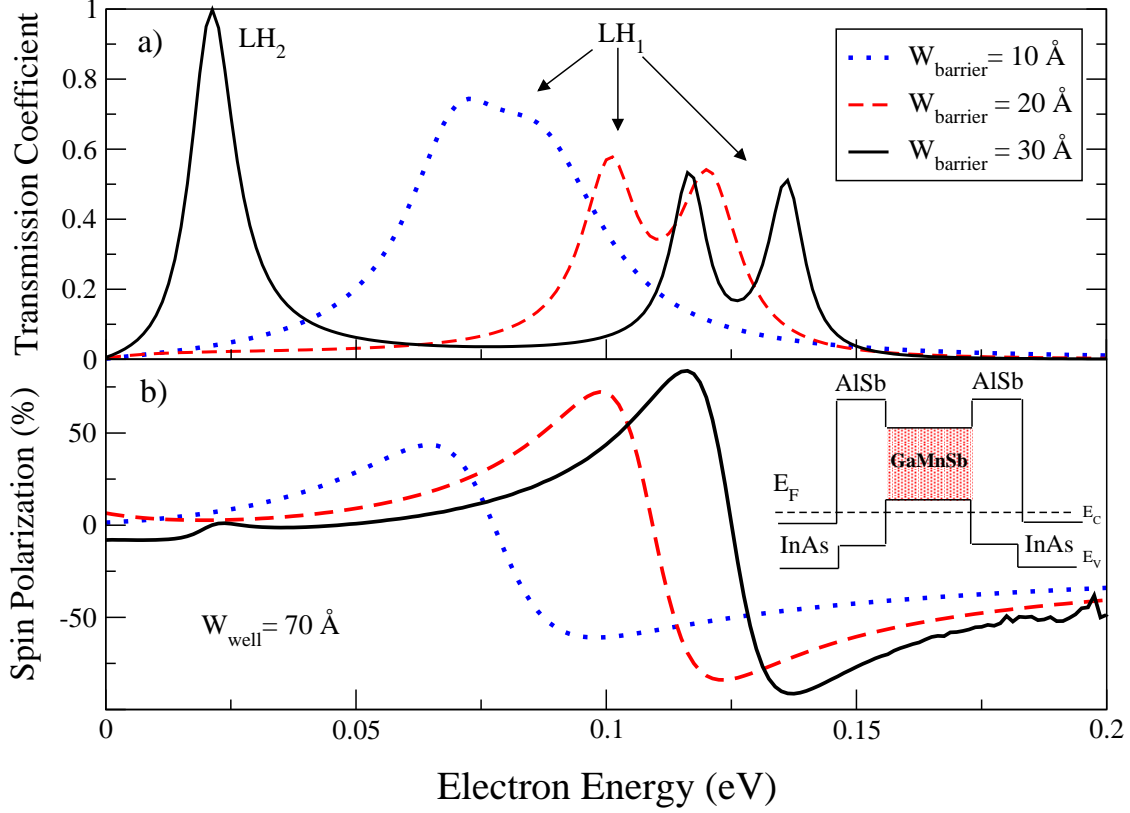


FIG. 1: (a) Transmission coefficients of InAs/AlSb/GaMnSb heterostructure with 70 \AA quantum well and various barrier widths; (b) Perpendicular single-electron spin polarizations at $\vec{k}_{\parallel} = 0$

DBH with the latter having an obvious advantage of being ferro- rather than paramagnetic. $\text{Ga}_{1-x}\text{Mn}_x\text{Sb}$ random alloys with Curie temperature $T_c \sim 25\text{-}30 \text{ K}$ have been grown and characterized [14]. Recently, much higher T_c has been reported for $\text{Ga}_{1-x}\text{Mn}_x\text{Sb}$ digital alloys [15]. At the same time, digital growth techniques are proven to be very efficient for growing high quality magnetic quantum wells [16]. This makes manufacturing of GaMnSb-based spin-RITDs a technological reality.

To describe spin-dependent interband resonant tunneling in GaMnSb-based DBH we use standard $8 \times 8 \mathbf{k} \cdot \mathbf{p}$ Kane Hamiltonians in the nonmagnetic InAs and AlSb regions [17] and a generalized Kane Hamiltonian which accounts for magnetism in $\text{Ga}_{1-x}\text{Mn}_x\text{Sb}$ quantum well:

$$H = H_e + H_h + H_{eh}. \quad (1)$$

Here $H_e = (\hbar^2 k^2 / 2m^*)I$ is the electron Hamiltonian, I is 2×2 unit matrix and we completely neglect a small exchange splitting of the conduction band in $\text{Ga}_{1-x}\text{Mn}_x\text{Sb}$. The second term

in Eq.(1) is the “Kohn-Luttinger+exchange” hole Hamiltonian [18, 19]:

$$H_h = H_{KL} + \frac{3}{2}\Delta_{ex}(\vec{\sigma} \cdot \hat{m}), \quad (2)$$

where $\vec{\sigma} \equiv (\sigma_x, \sigma_y, \sigma_z)$, σ_α are Pauli matrices, \hat{m} is the unit vector in the direction of magnetization, H_{KL} is a standard 6×6 Kohn-Luttinger Hamiltonian for GaSb [17], and Δ_{ex} is the exchange splitting of the light holes at $\vec{k} = 0$. We will consider only saturation magnetizations where $\Delta_{ex} = (5/6)\beta N_0 x$. Here β is the $p-d$ exchange coupling constant, N_0 is the number of cations per unit volume in $\text{Ga}_{1-x}\text{Mn}_x\text{Sb}$, and x is Mn concentration. The numerical value of $\Delta_{ex} \simeq 30$ meV at $x = 0.05$ is consistent with the Curie temperature of bulk GaMnSb [14, 19] $T_c \simeq 25\text{-}30$ K. The third term in Eq.(1) describes electron-hole coupling:

$$H_{eh}^\sigma = P \sum_{\alpha=x,y,z} k_\alpha (|\alpha\sigma\rangle\langle s\sigma| + |s\sigma\rangle\langle \alpha\sigma|), \quad (3)$$

where P is Kane’s parameter related to the matrix elements of the linear momentum operator $(m/\hbar)P = \langle s|p_x|x\rangle = \langle s|p_y|y\rangle = \langle s|p_z|z\rangle$, and $|s\rangle$ and $|\alpha\rangle$ are $\vec{k} = 0$ Bloch functions of the conduction and valence states respectively. We assume that z -axis is perpendicular to the layers.

To calculate the transmission coefficient we will use the transfer matrix technique [20] and represent the device as a stack of two-dimensional flat-band interior layers with thickness $w_n = z_n - z_{n+1}$ and an average electrostatic potential $-eV_n$ starting at $z = z_0 = 0$ and ending at $z = z_N$, where z_N is the length of the device. The $0_{th} \equiv L$ and $(N+1)_{th} \equiv R$ layers are semi-infinite InAs emitter ($z < 0$) and collector ($z > z_N$) having electrostatic potentials $V_0 = 0$ and $-eV_{N+1} = -eV$ respectively, where V is the bias applied to the structure. We will take into account elastic processes only, i.e. assume that the electron energy E and lateral momentum \vec{k}_\parallel are conserved. Substituting $k_z \rightarrow -i\hbar\partial/\partial z$ into the Kane Hamiltonian one can solve the Schrödinger’s equation in the n_{th} flat-band region:

$$\Psi_n(z) = \sum_{\alpha=1}^8 [A_{n\alpha}^+ v(k_{n\alpha}) e^{ik_{n\alpha}z} + A_{n\alpha}^- v(k_{n\alpha}) e^{-ik_{n\alpha}z}] \quad (4)$$

This formula reflects the fact that the complex eigenvalues $\pm k_{n\alpha}$ always occur in pairs. The technique of finding $\pm k_{n\alpha}$ and eigenvectors $v(\pm k_{n\alpha})$ is described in [20]. Using these quantities and the matching conditions ensuring wave function and current continuity across the device, we can construct the transfer matrix M which relates the the wave-function

amplitudes in the emitter and collector:

$$\begin{pmatrix} A_L^+ \\ A_L^- \end{pmatrix} = \begin{pmatrix} M_+ & M_{+-} \\ M_{-+} & M_- \end{pmatrix} \begin{pmatrix} A_R^+ \\ 0 \end{pmatrix} \quad (5)$$

The 16×16 matrix M in Eq. (5) is partitioned in such a way that M_+ expresses the amplitudes of the incident waves in the emitter A_L^+ through those of the transmitted waves A_R^+ in the collector. The collector wavefunction is a superposition of these waves that are either traveling solutions moving to the right (electron states) or evanescent solutions decaying to the right (hole states).

For any k_{\parallel} , E , and $-eV$, the 8×8 transfer matrix M_+ can be found and the transmission matrix can be calculated straightforwardly:

$$t_{\sigma\sigma'} = \begin{cases} \sqrt{j_{R\sigma'}/j_{L\sigma}} (M_+)_{\sigma'\sigma}^{-1}, & \text{if } j_{L\sigma} > 0 \text{ and } j_{R\sigma'} > 0 \\ 0, & \text{otherwise} \end{cases} \quad (6)$$

where $j_{L\sigma(R\sigma)}$ is the matrix element of the current operator for the electron with spin σ in the emitter (collector) [20]. The transmission coefficient $T(\vec{k}_{\parallel}, E, eV)$ and spin transmissivity $\vec{\mathcal{S}}(\vec{k}_{\parallel}, E, eV)$ [21] can be calculated as well:

$$T(\vec{k}_{\parallel}, E, eV) = \text{Tr}(t \cdot t^\dagger) \quad (7)$$

$$\vec{\mathcal{S}}(\vec{k}_{\parallel}, E, eV) = \text{Tr}(t \cdot \vec{\sigma} \cdot t^\dagger) \quad (8)$$

The transmission coefficients for InAs/AlSb/GaMnSb DBH with 70 Å-wide quantum well and 10, 20, and 30 Å-wide barriers are shown in Fig. 1 (a). The magnetization is saturated and directed along z -axis, i.e. perpendicular to the layers. The spin splitting of the LH channels is well pronounced for the structure with wider barriers (20 and 30 Å). It is weakly resolved as a shoulder for the structure with 10 Å barriers. The barrier width, which is responsible for the width of the spin-resolved peaks is therefore one of the critical parameters for the structures in question. This observation is well supported by the calculated single-electron perpendicular spin polarizations \mathcal{S}_z/T at $k_{\parallel} = 0$, shown in Fig. 1 (b) for 70 Å-wide quantum well and 10, 20, and 30 Å-wide barriers. The maximum value of p is 60% for the structure with 10 Å barriers, while for the structure with 30 Å barriers it reaches 95%.

Similarly to the conventional InAs/GaSb RITDs the heavy hole (HH) resonant peaks are absent at $\vec{k}_{\parallel} = 0$. For perpendicular (or zero) magnetization and a tunneling electron with

$k_{\parallel} = 0$, the z -component of the total angular momentum, J_z , is a good quantum number and, therefore, must be conserved. Thus, tunneling of s -electrons near the conduction band minimum of InAs with $J_z = \pm 1/2$ through the hole states with $J_z = \pm 3/2$ is prohibited. Such a possibility exists for either finite k_{\parallel} or in-plane magnetization. As we will see below the former is rather insignificant while the latter affects the interband resonant tunneling in a drastic way. For better insight we will treat our system by means of the tunneling Hamiltonian formalism [22] which gives an analytical expression for the transmission coefficient at $\vec{k}_{\parallel} = 0$. In this framework the system is described by two coupled Schrödinger equations:

$$H_{\sigma}^e |\psi_{\sigma}^e\rangle + \sum_m \hat{V}_{\sigma m} |\varphi_m^h\rangle = E |\psi_{\sigma}^e\rangle \quad (9)$$

$$\sum_{m'} H_{mm'}^h |\varphi_{m'}^h\rangle + \sum_{\sigma} \hat{V}_{m\sigma}^{\dagger} |\psi_{\sigma}^e\rangle = E |\varphi_m^h\rangle, \quad (10)$$

Eq. (9) describes an electron with spin $\sigma = \pm 1/2$ tunneling through the potential barrier (evanescent channel) which is coupled with the confined hole states φ_m^h by a mixing potential $\hat{V}_{\sigma m}$. The basis of the localized hole states $|\varphi_m^h\rangle$ is defined in terms of spherical harmonics with m being the z -projection of the angular momentum onto the interface normal. Thus matrix $H_{mm'}$ is non-diagonal for an arbitrary orientation of the magnetization with respect to the interface. At $\vec{k}_{\parallel} = 0$ the operator $\hat{V}_{\sigma m} = -i\hbar P \delta_{\sigma,m} \partial/\partial z$. Since H_{σ}^e has continuous spectrum the situation is typical for the appearance of Fano resonances [23].

We will concentrate on the two particularly important cases of magnetization perpendicular and parallel to the layers. Taking into account only the first two quantized hole levels $E_{1/2}$ (light hole) and $E_{3/2}$ (heavy hole) and assuming that the barrier is symmetric (i. e. $eV = 0$), we obtain the the following expression for the transmission coefficient at $k_{\parallel} = 0$:

$$T_{\hat{m}}(E) = \frac{1}{2} T_0 \sum_{\sigma=\pm 1} \frac{(\Sigma_{\hat{m}}^{\sigma}(E) + \Delta_E)^2}{\left(\Sigma_{\hat{m}}^{\sigma}(E) + \Delta_E - \Gamma_E \sqrt{R_0/T_0}\right)^2 + \Gamma_E^2} \quad (11)$$

where $T_0 = |t_0|^2$ and $R_0 = 1 - T_0$ are the “bare” transmission and reflection coefficients, describing non-resonant and spin-independent electron tunneling in the absence of the mixing potential, and the self-energy $\Sigma_{\hat{m}}^{\sigma}(E)$ is given by:

$$\Sigma_{\hat{m}}^{\sigma}(E) = \begin{cases} E - E_{1/2} - \frac{1}{2}\sigma\Delta_{ex}, & \hat{m} \parallel z \\ E - E_{1/2} - \sigma\Delta_{ex} - \frac{3\Delta_{ex}^2}{4(E - E_{3/2})}, & \hat{m} \parallel x \end{cases} \quad (12)$$

Here we have introduced the inverse elastic life-time of the light-hole state $\Gamma_E \propto P^2$ and its energy shift due to the mixing potential $\Delta_E \propto P^2$. The expressions for Γ_E and Δ_E can be

obtained straightforwardly, however they are rather cumbersome and not important for our analysis. The only fact which is important is that both Γ_E and Δ_E are decreasing functions of the barrier width.

Eq. (12) allows for rather meaningful and physically transparent interpretation of the transmission coefficient, calculated numerically by means of the transfer matrix technique (Fig. 2). First of all we note that Eq. (12) describes a series of Fano resonances and antiresonances [23, 24, 25]. In the absence of the magnetization, $\Sigma_+(E) = \Sigma_-(E) = \Sigma(E)$ and we have only one resonance ($T(E) = 1$) at $\Sigma + \Delta_E = (\Gamma_E/2) \sqrt{T/R}$ and anti-resonance ($T(E) = 0$) at $\Sigma(E) + \Delta_E = 0$, both corresponding to the light-hole channel. When the magnetization \vec{M} is perpendicular to the layers, the light-hole (LH) resonance is exchange split which leads to the perpendicular spin polarization of the transmitted electron wave. Finally, the in-plane magnetization splits LH channel even more strongly and induces another resonance-antiresonance pair corresponding to the heavy hole (HH) channel. This chan-

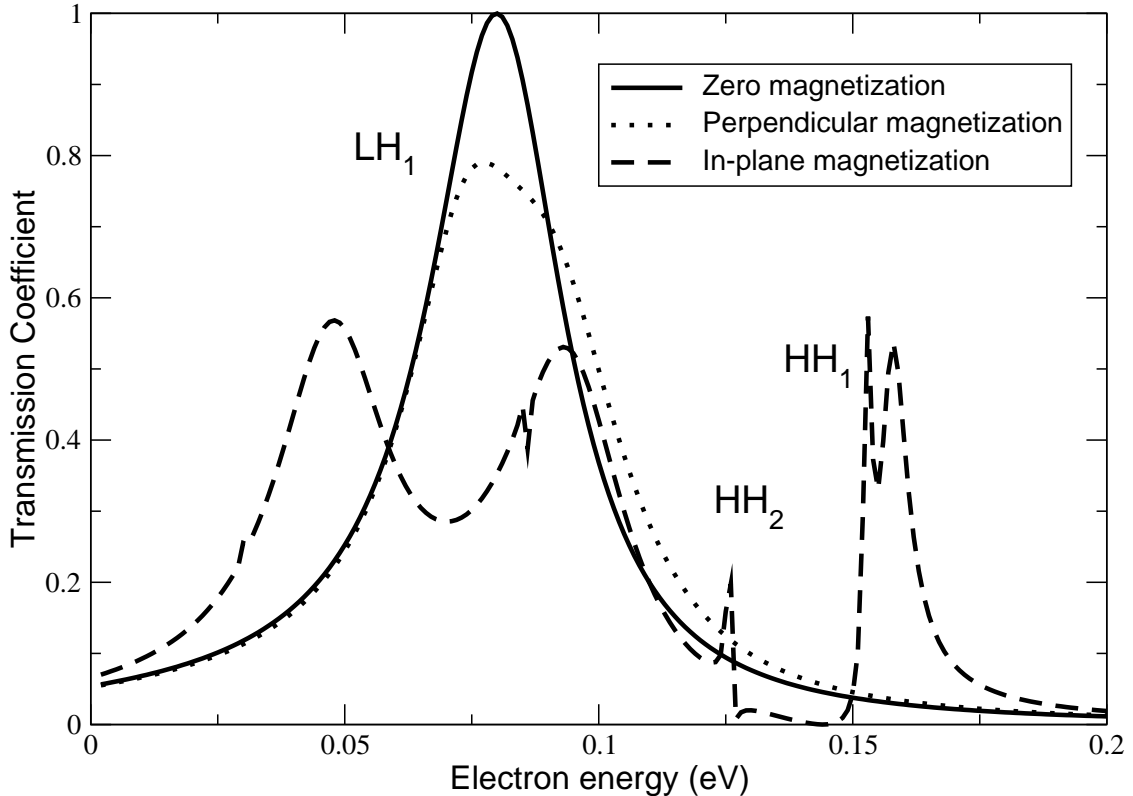


FIG. 2: Transmission coefficients of InAs/AlSb/GaMnSb DBH with 70 Å quantum well and 10 Å barriers ($\vec{k}_{\parallel} = 0$).

nel, which is completely invisible for zero or perpendicular magnetization, becomes very pronounced when \vec{M} is in-plane. This is a direct manifestation of the angular momentum selection rules combined with the exchange enhancement of the effective g -factor due to the localized Mn spins in the quantum well [18, 26].

We now turn to a calculation charge j and spin \vec{j}_s current densities [27]:

$$j = \frac{e}{4\pi^2\hbar} \iint d\vec{k}_{\parallel} dE [f(E) - f(E + eV)] T(\vec{k}_{\parallel}, E, eV) \quad (13)$$

$$\vec{j}_s = \frac{e}{4\pi^2\hbar} \iint d\vec{k}_{\parallel} dE [f(E) - f(E + eV)] \vec{\mathcal{S}}(\vec{k}_{\parallel}, E, eV), \quad (14)$$

where $f(E)$ is the Fermi function. Current-voltage characteristics calculated for $T=4$ K, 20 Å barriers and a 70 Å quantum well are shown in Fig. 3 (a). The current is calculated for perpendicular magnetization and the Fermi energy $E_F = 0.04$ eV, which corresponds to electron concentration in InAs $n \sim 10^{18} \text{cm}^{-3}$, and 0.1 hole per Mn ion in the $\text{Ga}_{1-x}\text{Mn}_x\text{Sb}$ quantum well at $x = 0.05$. The exchange splitting of the LH channel is resolved as a shoulder on the total current curve, which is a superposition of two very distinct partial spin-up and spin-down currents. This suggests that perpendicular spin polarization $j_{s,z}/j$ of the tunneling current must be quite significant (Fig. 3 (b)). In this particular case (20 Å barriers) $j_{s,z}/j$ reaches 90%. The most striking result of our calculations is a sharp dependence of spin polarization on the applied bias. As follows from Fig. 3 (b), one can drastically change both magnitude and sign of $j_{s,z}/j$ by applying external voltage. Such controllable spin filtering is a remarkable feature of magnetic RITDs and may have significant potential for a variety of possible spin-injection applications [28]. Since the spin-split channels are better resolved for the structures with wider barriers (Fig. 1) the spin polarization of the tunneling current is also higher for these structures. However, this effect is not as strong as we might expect, and the highest polarization values for different barrier widths are rather similar (Fig. 3 (b)).

As we already mentioned, the in-plane magnetization affects resonant tunneling in a dramatic way (Fig. 2). Fig. 4 shows three current-voltage characteristics for zero, perpendicular, and parallel magnetizations, calculated for $T = 4$ K and the structure with 70 Å quantum well and 10 Å barriers. The zero magnetization curve is similar to that of the conventional RITDs and displays a very strong LH resonant channel and a very weak feature stemming from the first HH state in the quantum well. The same is true for the perpendicular magnetization where the LH channel is split into spin-up and spin-down subchannels but

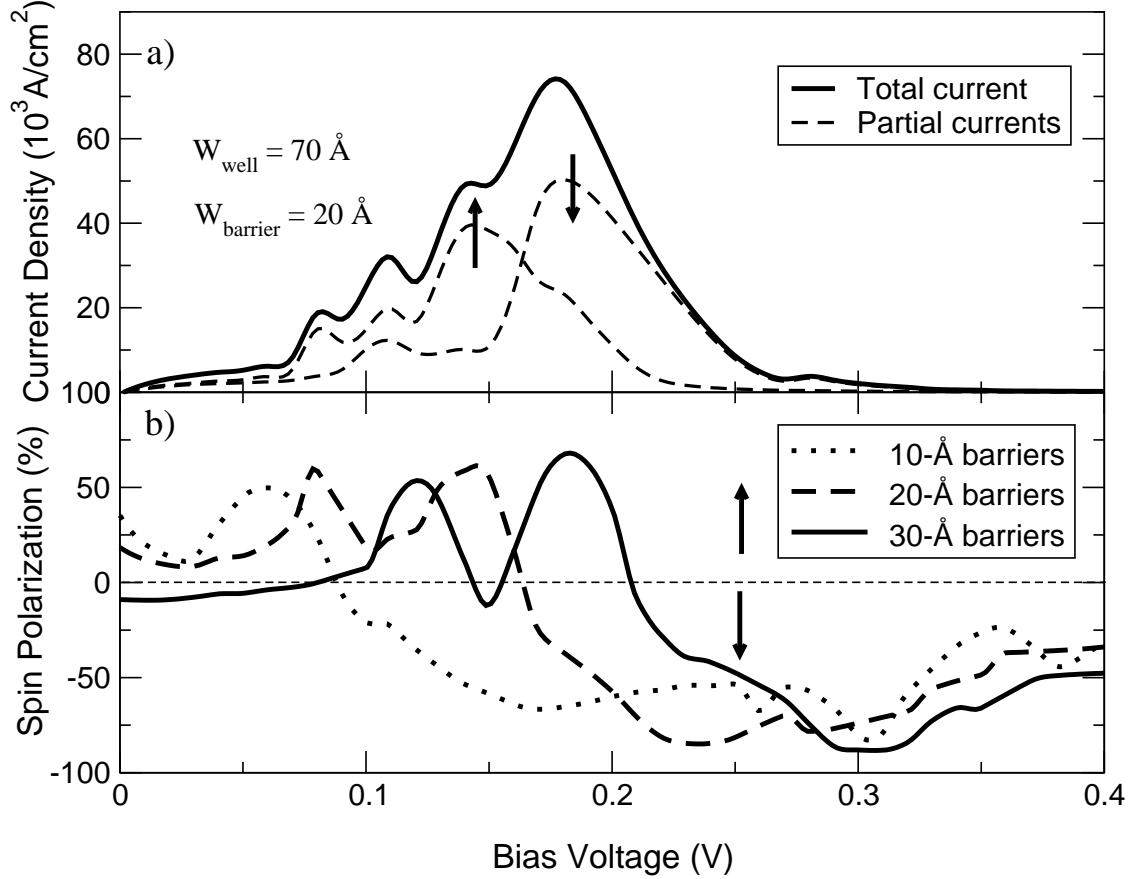


FIG. 3: a) I-V curve for InAs/AlSb/GaMnSb DBH with 70 \AA quantum well, 20 \AA barriers, and perpendicular magnetization; b) bias dependence of the current spin polarization $j_{s,z}/j$ for 70 \AA quantum well, various barriers and perpendicular magnetization.

the HH peak remains very weak. The most drastic changes of the $I - V$ characteristics occur for the in-plane magnetization where, along with the splitting of the light-hole channel, two new peaks related to the heavy hole states in the quantum well emerge. This effect is due to the mixing of the LH and HH channel at $\vec{k}_{\parallel} \simeq 0$ which results in the lifting of the angular momentum selection rules [18]. The induced heavy-hole resonant channels have been clearly observed in resonant tunneling through paramagnetic ErAs quantum wells in saturating in-plane magnetic fields [13]. Even though nonzero k_{\parallel} in the cases of perpendicular and zero magnetization also allows for tunneling of the electrons through the heavy-hole states, the corresponding resonances are rather weak, and are almost completely washed out by the integration over k_{\parallel} in Eq. (13) (see also Ref. [8]).

This work is supported by NSF Grant No 0071823 and by NRL under ASEE-NAVY

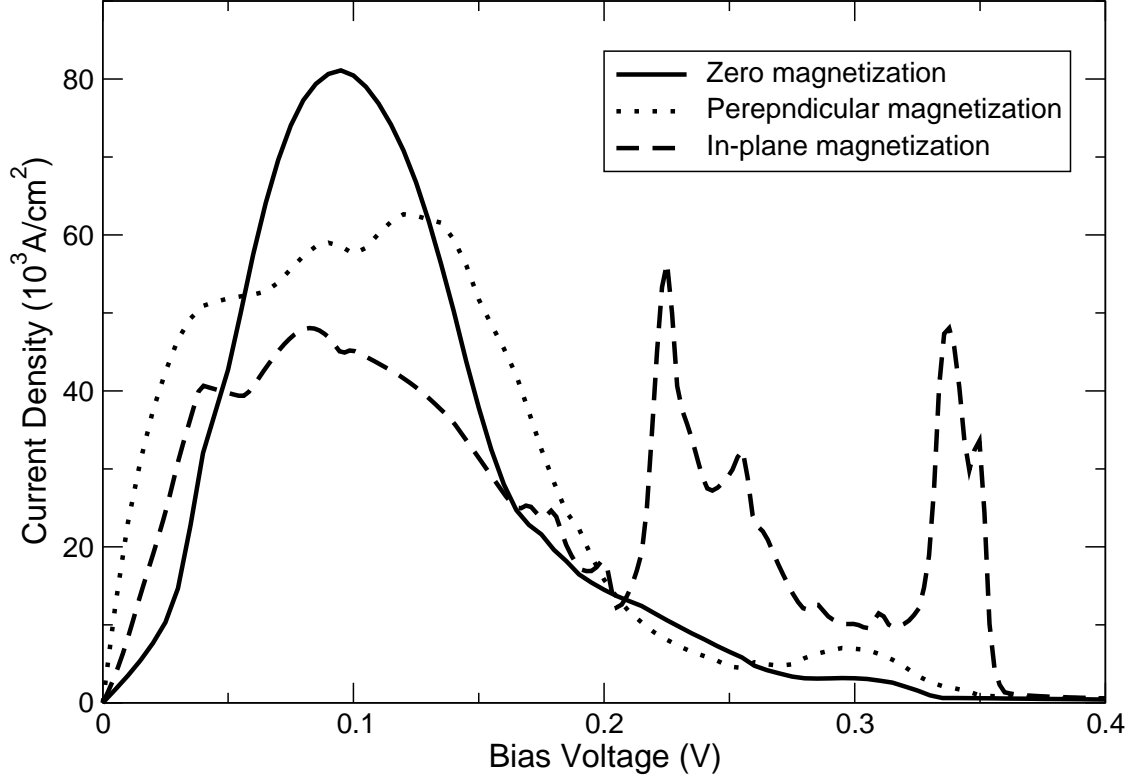


FIG. 4: $I - V$ charactersitics of InAs/AlAs/GaMnSb DBH with 70 Å quantum well and 10 Å barriers, for zero, perepndicular and in-palne magnetizations in the quantum well.

Summer Faculty Program.

-
- [1] E. I. Rashba, Phys. Rev. B **62**, R16267 (2000).
 - [2] H. J. Zhu, M. Ramsteiner, H. Kostial, M. Wassemeir, H.-P. Schonherr, and K. H. Ploog, Phys. Rev. Lett. **87**, 016601 (2001).
 - [3] A. T. Hanbicki, B. T. Jonker, G. Itskos, G. Kiioseoglou, and A. Petrou, Appl. Phys. Lett. **80**, 1240 (2002).
 - [4] T. Koga, J. Nitta, H. Takayanagi, and S. Datta, Phys. Rev. Lett. **88**, 126601 (2002).
 - [5] M. Kohda, Y. Ohno, K. Takamura, F. Matsukura, and H. Ohno, Jpn. J. Appl. Phys. **40**, L1274 (2001).
 - [6] E. Johnston-Halperin, D. Lofgreen, R. K. Kawakami, D. K. Young, L. Coldren, A. C. Gossard, and D. D. Awschalom, Phys. Rev. B **65**, 041306 (2002).

- [7] J. M. Kikkawa and D. D. Awschalom, *Nature (London)* **397**, 139 (1999).
- [8] Y. X. Liu, R. R. Marquardt, D. Z.-Y. Ting, and T. C. McGill, *Phys. Rev. B* **55**, 7073 (1997).
- [9] R. R. Marquardt, D. A. Collins, Y. X. Liu, D. Z.-Y. Ting, and T. C. McGill, *Phys. Rev. B* **53**, 13624 (1996).
- [10] E. E. Mendez, J. Nocera, and W. I. Wang, *Phys. Rev. B* **45**, 3910 (1992).
- [11] E. E. Mendez, *Surf. Sci.* **267**, 370 (1992).
- [12] T. Takamasu et al., *Surf. Sci.* **263**, 217 (1992).
- [13] D. E. Brehmer, K. Zhang, C. J. Schwarz, S. P. Chau, and S. J. Allen, *Appl. Phys. Lett.* **67**, 1268 (1995).
- [14] F. Matsukura, E. Abe, and H. Ohno, *J. Appl. Phys.* **87**, 6442 (2000).
- [15] X. Chen, M. Na, S. Wang, H. Luo, B. D. McCombe, X. Liu, Y. Sasaki, T. Wojtowicz, J. K. Furdyna, S. J. Potashnik, et al., *Appl. Phys. Lett.* **81**, 511 (2002).
- [16] S. A. Crooker, D. A. Tulchinsky, J. Levy, D. D. Awschalom, R. Garcia, and N. Samarth, *Phys. Rev. Lett.* **75**, 505 (1995).
- [17] D. N. Talwar, J. P. Loehr, and B. Jogai, *Phys. Rev. B* **49**, 10345 (1994).
- [18] A. G. Petukhov, W. R. L. Lambrecht, and B. Segall, *Phys. Rev. B* **53**, 3646 (1996).
- [19] T. Dietl, H. Ohno, F. Matsukura, J. Cibert, and D. Ferrand, *Science* **287**, 1019 (2000).
- [20] A. G. Petukhov, A. N. Chantis, and D. O. Demchenko, *Phys. Rev. Lett.* **89**, 107205 (2002).
- [21] J. C. Slonczewski, *Phys. Rev. B* **39**, 6995 (1989).
- [22] S. A. Gurvitz and Y. B. Levinson, *Phys. Rev. B* **47**, 10578 (1993).
- [23] U. Fano, *Phys. Rev.* **124**, 1866 (1961).
- [24] R. C. Bowen, W. R. Frensley, G. Klimeck, and R. K. Lake, *Phys. Rev. B* **52**, 2754 (1995).
- [25] G. Klimeck, R. C. Bowen, and T. B. Boykin, *Superlattices and Microstructures* **29**, 187 (2001).
- [26] A. G. Petukhov, *Appl. Surf. Sci.* **123/124**, 385 (1998).
- [27] C. B. Duke, *Tunneling in Solids* (Academic, 1969).
- [28] G. A. Prinz, *Science* **250**, 1092 (1990).